FLOW CELL STUDIES ON FOULING CAUSED BY PROTEIN -CALCIUM PHOSPHATE DEPOSITION IN TURBULENT FLOW

R. Rosmaninho[1], G. Rizzo[2], H. Muller-Steinhagen[2] and L. F. Melo[1]
[1] LEPAE, Departamento de Engenharia Química, Universidade do Porto, Rua Dr. Roberto Frias, 4200-465 Porto, Portugal
[2] Universität Stuttgart, ITW Institut für Thermodynamik und Wärmetechnik, Pfaffenwaldring 6, D-70550 Stuttgart, Germany
E-mail: lmelo@fe.up.pt

ABSTRACT

A comparative study of the calcium phosphate fouling process, with and without proteins, was carried out using both standard 316 2R stainless steel and 2R surfaces modified by TiN magnetron sputtering. Fouling behavior was assessed in a heat transfer flow cell operating in the turbulent flow regime. The fouling curves resulting from calcium phosphate deposition in the absence of proteins were substantially different from the ones obtained when protein was present. In this last case, two different fouling periods could be observed. The surface energy of the modified materials was found to affect the deposition parameters (rate of deposition and final amount of deposit) leading to higher amounts of deposit on higher energy surfaces in the absence of protein, while leading to less deposit in its presence. The standard 316 2R substrate proved to be less prone to fouling from protein-calcium phosphate solutions than the TiN modified surfaces. However, the same conclusion could not be drawn for calcium phosphate solutions.

INTRODUCTION

The importance of the study of the fouling behavior from solutions containing calcium phosphate and whey proteins emerges from the fact that these milk components constitute the two major mechanisms of fouling during the heat treatment of milk, since fouling results respectively from protein denaturation and from the precipitation of calcium phosphate upon heating. The two phenomena seem to be connected since calcium ions not only contribute to the process through calcium salt deposition, but also have a significant influence on denaturation and aggregation of the proteins prior to deposition (Bansal and Chen, 2006; Jeurnink et al., 1996).

Recent work from Morison and Tie on milk simulating solutions (2002) proved that fouling is mainly caused by surface reactions of both calcium phosphate and protein. In the initial stages of milk processing, individual whey protein molecules are adsorbed onto the stainless steel heating surface covering most of the surface with a protein monolayer, after which the deposition of aggregates formed in the bulk, both as calcium phosphate and as whey protein particles**,** occurs (Visser and Jeurnink, 1997). Consequently, it seems that proteins are the ones to start the fouling process, as hypothesized by Morison and Tie (2002) and by Belmar-Beiny and Fryer (1993), who stated that the modification of the surface properties could be responsible for changing the number and type of bonds between the protein and the surface. The formation of the first protein deposition layer is known to be affected by several factors, related to both the nature of the heating surface and the bulk solution properties. The influence of surface characteristics on whey protein adsorption was studied by Santos et al. (2006) and previously by Adesso and Lund (1997) but even though the surface was considered an important parameter in each case, no direct relationship was found between surface energy parameters and the adsorption process.

In the fluid bulk, calcium ions promote β-lactoglobulin aggregation and stabilization by binding between adjacent carboxyl groups. Consequently, the presence of whey protein in solution will tend to retard the crystallization process of calcium phosphate (Tsuge et al., 2002). Once on the surface, the calcium ions form bridges between the first adsorbed proteins and the protein aggregates formed in the solution, thereby promoting the subsequent fouling stages. In some studies, however, the addition of calcium seemed to decrease fouling caused by a whey protein concentrate which even became negligible for some temperature ranges (Christian et al., 2002). These apparently contradictory findings suggest that the interferences between protein and mineral components depend also on the stage of fouling considered.

An understanding on how the two components are affected by the surface properties can be a significant step forward in the search for a surface able to reduce fouling in dairy processing equipment. Consequently, the present work is focused on the interrelation between the fouling behaviors of whey proteins and calcium phosphate under turbulent flow on different stainless steel modified surfaces.

MATERIALS AND METHODS

Calcium Phosphate with and without milk proteins

The foulant solution used in this work was SMUF (Simulated Milk Ultra Filtrate), which is an aqueous solution that has been used to study the deposition of calcium phosphate. SMUF was prepared according to Jenness and Koops (1962) and kept overnight at 5ºC for stabilization before use. Another aqueous solution (here called Modified SMUF or "MOD-SMUF") was also prepared in order to study the effect of whey protein on the deposition behavior of calcium phosphate,. To prepare this solution, a commercial WPI (Whey Protein Isolate, Lacprodan DI-9224) provided by Arla Foods (Arla Foods, Ingredients, Denmark) was added to the SMUF solution in order to obtain 3g/l of β-lactoglobulin (β-lg). The pH of both solutions was adjusted to 6.80 using dilute NaOH.

TiN Surfaces and Its Preparation by Reactive Magnetron Sputtering

To isolate the influence of the surface energy of the substrate on the fouling process from all the other affecting parameters, different stainless steel based surfaces with a wide range of surface energies, but similar roughness and qualitative chemical compositions, were produced at the University of Stuttgart. All surfaces were 316 2R (bright annealed) based and were prepared by using a surface modification technique called reactive magnetron sputtering, as explained in detail in (Rosmaninho et al., accepted for publication). Because this is a coating technique, all the surfaces became covered by a similar layer of TiN which differed only on the surface energy. The surfaces were named TiN 1, TiN 2, TiN 3, TiN 4 and TiN 5 and the non-modified 316 2R surface was used as control. Each sample had 15 x 60 x 1 mm as dimensions.

Surface Characterization

X-ray Photoelectron Spectroscopy (XPS)

The chemical composition of the outer layers of all the modified surfaces was measured by XPS. The XPS analysis was performed using ESCALAB 200A, VG Scientific (UK). For analysis, an achromatic Al X-ray source operating at 15kV (300 W) was used. The spectrometer calibrated with reference to Ag 3d5/2 (368.27 eV) was operated in CAE mode with 20eV pass energy. Spectra analysis was performed using peak fitting with Gaussian-Lorentzian peak shape and Shirley type background subtraction.

Surface Energy Characterization

Contact angle values were measured by the sessile drop method in a contact angle meter (DataPhysics OCA15 Plus, Germany) using water, formamide and α-bromonaphtalene as reference liquids. The contact angles were measured automatically using an image analyzing system. Contact angle measurements were performed on every stainless steel sample 24h after being cleaned with a commercial detergent (RBS35 from RBS Chemical Products). For each sample at least 15 measurements with each liquid were performed covering the whole sample surface.

The surface energy of each sample was determined based on the contact angle values and following the Lewis acid-base theory (van Oss, 1994). This theory evaluates the total surface energy of a solid (γ^{TOT}) as the sum of an apolar Lifshitz-van der Waals component (γ^{LW}) and an acid-base polar component (γ^{AB}):

$$\gamma^{TOT} = \gamma^{LW} + \gamma^{AB} \quad (1)$$

The last one, γ^{AB}, is composed of two non-additive parameters, one for the electron donor component (γ^{-}) and one for the electron acceptor (γ^{+})as follows (van Oss, 1994):

$$\gamma^{AB} = 2\sqrt{\gamma^{+}\gamma^{-}} \quad (2)$$

Deposition and Cleaning Experiments

Heat Flow Cell

Figure 1 presents the scheme of the continuous flow rig that was set up to follow the evolution of the thermal resistance of the deposits formed on the different stainless steel surfaces. The equipment consisted of: a) a well stirred stainless steel tank of 120 L containing the foulant solutions (SMUF and MOD-SMUF), which was kept at constant temperature by a resistance coil with an on-off temperature controller; b) a smaller tank for heating the oil used as heating medium; c) a data acquisition board with a sensor interface card (UPC 2100, Valiyne Engineering) connected to a computer operating with a Labtech program (Measurement Computing Corporation) for temperature acquisition, processing and recording; and d) the vertical fouling test section (Flow Cell) where the different samples were placed and where the overall heat coefficient was measured (Figure 2).

In the fouling experiments, the foulant solutions was pumped through the flow cell to generate fouling and returned to the tank. The flow velocity was controlled by a calibrated rotameter. The oil, used as the heating medium, was channeled along the back of the fouling test section and recycled to the oil tank.

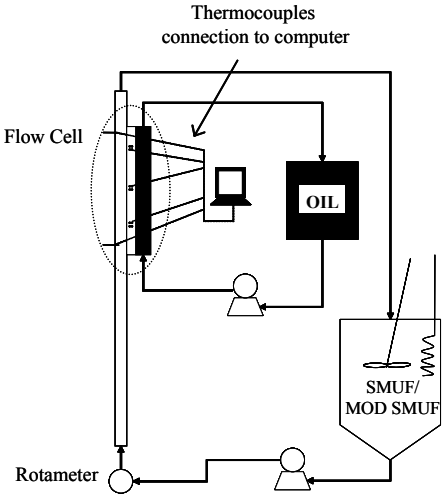

Figure 1: Schematic diagram of the heat flow cell

The Flow Cell cross-section is semi-circular with a diameter of 0.03 m. The total length of the flow cell is 1.53 m and the fouling measuring section is placed 1.0 m after the entrance to allow complete boundary layer development for turbulent flow conditions (Incropera, 1992). The stainless steel rectangular samples are imbedded in a stainless steel plate parallel to the flow and sufficiently separated from each other to avoid possible interferences. The experiments were performed in triplicate for each run (Figure 2b). To evaluate the temperature along the surface under the sample, a pair of thermocouples (Type E, Omega Engineering, Inc.) was inserted into the stainless steel plate at two different locations (T_2 and T_3 in Figure 2a). For better reliability, the measurements were performed in the two extremes of the sample (Figure 2b). The SMUF temperature in the flow cell was considered as the average value obtained by two thermocouples (Type E, Omega Engineering, Inc.), one at the inlet of the measuring section and another one at the outlet (T_1 in Figure 2a)

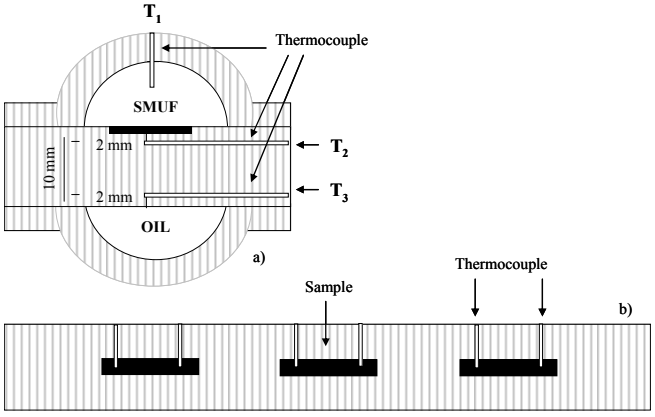

Figure 2: Detailed schematic diagram of the fouling test section: a) transversal view; b) longitudinal top view

Overall Heat Transfer Coefficient (U) and Fouling Resistance (R_f)

Deposit formation on a surface can be monitored by following the overall heat transfer coefficient (U) and the fouling resistance (R_f) along the process (Prakash et al., 2005).

For the present geometry, the overall heat transfer coefficient between thermocouple 3 and the SMUF solution is calculated by (3):

$$U = \frac{k}{x}\frac{\left(T_3 - T_2\right)}{\left(T_3 - T_1\right)} \qquad (3)$$

k is the thermal conductivity of the wall material, x the distance between the two thermocouples embedded in the wall (temperatures T_2 and T_3) and T_1 is the temperature of the solution.

As the fouling layer builds up, its thermal resistance is calculated as the difference between the overall thermal resistances for the initially clean surface ($\frac{1}{U_0}$) and for the fouled surface ($\frac{1}{U}$) according to equation (4):

$$R_f = \frac{1}{U} - \frac{1}{U_0} \qquad (4)$$

The fouling process can then be monitored by the evolution of R_f with time.

When the flow rate is kept constant, the presence of a deposit on the surface of a channel tends to increase the pressure drop due to the deposit roughness and, to a negligible extent, to the reduction of the cross-sectional flow area. Thus, fouling resistance and friction factor can be estimated by simultaneously monitoring the heat transfer and the pressure drop across the test section. In the present case, the increase in pressure drop measured between the inlet and outlet of the fouling test section was not detectable, probably because the relative roughness of the deposit formed was not significant. Consequently, only the heat transfer measurements were considered to calculate the fouling resistance.

Operating Conditions in the Flow Cell

The fouling experiments presented in this work comprised two stages: 1) evaluation of the overall heat transfer

coefficient with the clean surface. This stage was performed with water at the deposition conditions (same temperature, heat flux and fluid velocity) and 2) monitoring the change in the overall heat transfer coefficient during the fouling process. All experiments were carried out at a constant temperature of 48ºC for SMUF and 50ºC for MOD-SMUF corresponding to the beginning of bulk precipitation of calcium phosphate aggregates in each case. The heating medium used in the experiments was oil at a constant temperature of 70ºC which created an initial average temperature difference between the deposition surface and the foulant solution of 1.6ºC for SMUF and 1.5ºC for MOD-SMUF. Since the mass concentration of minerals in the SMUF solutions is as small as 0.8 %, SMUF physical properties can be considered identical to those of water at the same temperature. The deposition experiments were performed at a Reynolds number of 6 256 (flow velocity 0.20 m/s in the test section). The ambient temperature was controlled by air conditioning to a constant value of 25ºC during the whole experiment.

The solutions were prepared in the tank and kept at a constant temperature throughout the various experiments. They were also kept under constant agitation in order to avoid deposition on the base of the tank and to maintain a homogeneous temperature in the liquid. Their pH was adjusted to 6.80 (WTW inolab pH level1) at the beginning of the experiments but was allowed to vary along the experiment as a consequence of aggregate precipitation and/ or protein transformation. During the experiments, liquid samples were collected and vacuum filtered using a 0.45 μm filter in order to remove the aggregates formed in the supernatant. The pH of the collected samples as well as the free calcium concentration in solution was recorded along the process (WTW-D82362 Weitheim), as a way of evaluating the degree and type of the reactions occurring in the bulk.

Off-line Quantification and Characterization of the Deposit

After the experiments, the test section was dismantled and the samples were removed. The amount of deposit formed on each sample was determined by weighing the samples using an analytical balance (AND GR-200, AND Engineering, California, USA).

The structure of the deposits formed from each foulant solutions was characterized by scanning electron microscopy observation (JEOL JSM6301F, Japan), while their chemical composition was assessed by X-ray microanalysis (Noran Voyager, Noran Instruments Inc, USA).

RESULTS

Surface Characterization by Surface Energy Values

The surfaces used in this study were characterized based on their surface energy values and distinguished by their value for its electron donor component (γ-) as shown in Table 1.

Table 1 Surface energy components for 2R unmodified surfaces and for all TiN sputtered surfaces (standard deviation in brackets)

Surface	γ- (mJ/m^2)
2R	39,0 (3.1)
TiN 1	55.3 (0.0)
TiN 2	23.0 (1.8)
TiN 3	46.2 (4.6)
TiN 4	18.4 (2.7)
TiN 5	26.0 (2.2)

Deposition Process of Calcium Phosphate on 2R Surfaces

The repeatability of the fouling development and the reliability of the measuring technique were assessed by performing three trial runs (2R1, 2R2 and 2R3) on 2R surfaces. Each fouling curve, presented in Figure 3, represents the average value obtained for the three surfaces tested in each experiment (trial run). The reproducibility of the measurements was quite satisfactory and the evolution of the fouling resistances (R_f) with time was very similar for the three experiments, mainly in the earlier periods of fouling. After approximately 60 h of deposition, some differences were noticed mainly for the 2R3 test, most probably caused by differences in the bulk properties. These differences can be due to changes in the composition of the bulk liquid with time, since its properties (like calcium concentration and pH) were not controlled to a specific set-point but were only fixed initially and subsequently monitored.

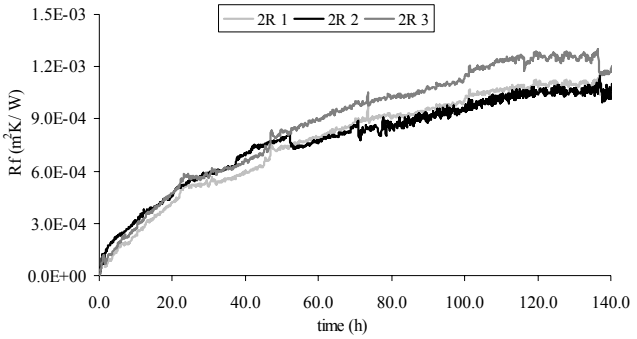

Figure 3: Fouling curve for three trials on 2R surfaces

Fouling Behavior of SMUF on the Different Surfaces

The fouling curves on the different studied surfaces are presented in Figure 4. Both the initial deposition behavior, obtained by the slope of the curves at the beginning of the deposition process and the stabilization (asymptotic) fouling values, were found to depend on the specific surface. The surfaces in Figure 4 are presented according to increasing surface energy (γ- value).

Coupled with the fact that no significant differences were observed in the bulk liquid, the data in Figure 4 seems to indicate that different processes take place at the different surfaces, influencing the subsequent deposition stages and hence the overall fouling process.

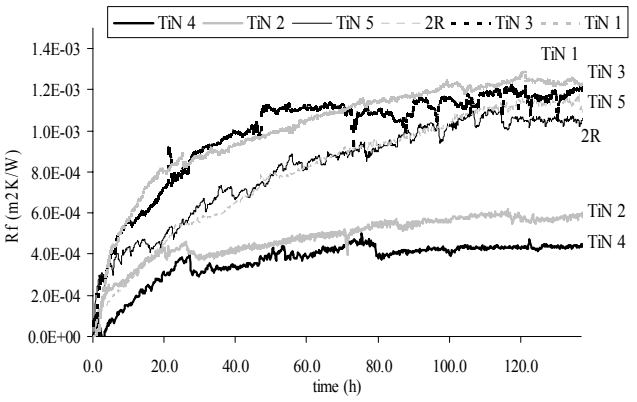

Figure 4: Fouling behavior on the different surfaces during the deposition period (surfaces are presented in the caption according to increasing γ- parameter)

Analyzing the fouling curves in Figure 4, the surfaces can clearly be divided into 2 groups: a) low surface energy (TiN 4 and TiN 2), presenting the lowest stabilization fouling resistance, and b) the medium and higher surface energy ones (TiN 5, 2R, TiN 3 and TiN 1) which stabilize at the highest fouling values. It can be said that under these conditions, deposition on the surfaces with lower γ- started to develop slower and finally reached a final lower amount, while the higher γ- surfaces produced a higher deposition rate and developed much more deposit at the end of the experiments. The explanation for such differences can be based on the size and number of the aggregates initially formed on the different surfaces, as previously presented for laminar regime deposition under batch conditions (Rosmaninho and Melo, 2006). Low γ- surfaces provide fewer adhesion points and present larger aggregates, while higher γ- surfaces present a higher number of smaller aggregates as a result of more adhesion points for the initial attachment and growth.

To better quantify the fouling process and more easily distinguish the fouling process between the different surfaces, a quantification of the initial deposition and the stabilization values was attempted.

Kern and Seaton (1959), in their simple model to describe the fouling process, considered a deposition rate (ϕ_d) and a detachment rate (ϕ_r) where the detachment rate is supposed to increase with time as a result of the lower cohesion of the outer layers. When assuming a constant deposition rate, the following equation can be used to describe the total fouling process.

$$Rf = Rf^{\infty}\left(1-\exp(-bt)\right) \qquad (5)$$

In this equation, Rf^{∞} represents the stabilization or asymptotic value for the fouling resistance (R_f) and b represents the proportionality constant between the deposition rate (ϕ_d) and Rf^{∞} as defined by

$$\phi_d = b\, Rf^{\infty} \qquad (6)$$

The deposition process for all the surfaces followed a similar trend and the experimental data could be fitted to the asymptotic equation shown above (equation 5). Two examples of the model fitting are presented in Figure 5, corresponding to the TiN 3 and TiN 4 surfaces, respectively, i.e. to a low and a high surface energy case.

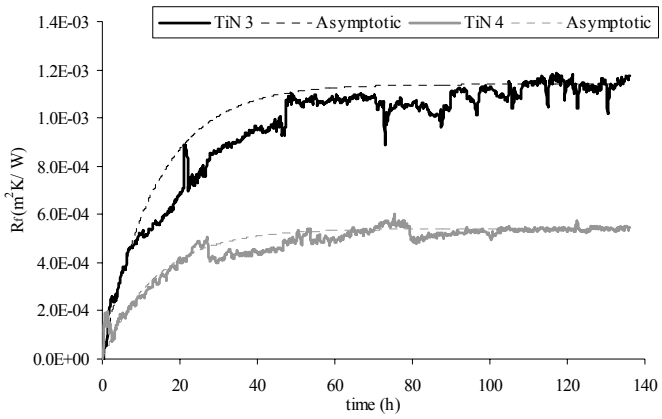

Figure 5: Asymptotic fitting of the fouling curves of a higher and a lower surface energy sample

The fit, even though not perfect during the intermediate period of the experiment, was rather good in the initial and final stages of deposition. Comparison between the deposition behaviors on the different surfaces will focus on the initial deposition rate and the Rf^{∞} value obtained by this approach. Figure 6 plots then the deposition rates and the Rf^{∞} values for each surface and shows that the maximum amount of deposit was higher for higher surface energies. In fact, an almost linear relationship between the γ- component of the substrate material and the final amount of deposit formed was found (Rosmaninho, 2007).

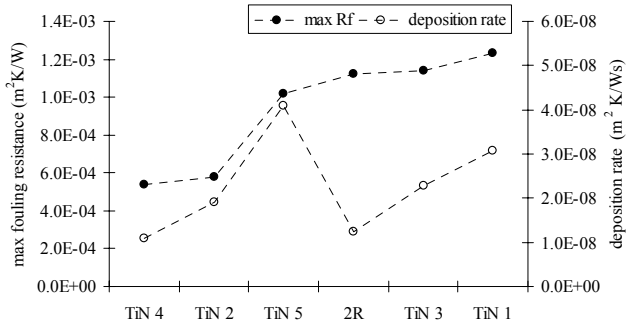

Figure 6: Deposition rates (ϕ_d) and maximum value of fouling resistance (Rf^{∞}) obtained for each surface after fitting an asymptotic model. Surfaces are indicated by increasing γ- component, from left to right.

In the same figure, a similar relationship with γ- can be found for the deposition rate and higher values were also obtained for the surfaces having higher γ- values. However, for the deposition rate, the relationship was not always increasing over the whole range of γ- values, since a very pronounced increase for the TiN 5 surface (γ- = 23) was followed by a return to the lowest value for the 2R surface (γ- = 39). No obvious explanation was found for this behavior, but it could be related to the fact that the TiN 5 surface has a much higher titanium (Ti) percentage (20-25 %) than all the other surfaces (8.1 % for TiN 4 and TiN2; 8.7 % for TiN 3 and TiN 1 and 10.4% for TiN 5, as measured with XPS). Nevertheless this property did not seem to affect significantly the surface energy it may have affected the initial interactions between surface and calcium phosphate. The low value of the initial deposition rate for the 2R surface can be related to the fact that the roughness of untreated stainless steel is smaller than that of surfaces treated by reactive sputtering (Santos et al., 2004).

Comparison between the Fouling Behavior of Calcium Phosphate with and without Proteins on Non-modified Surfaces

The deposition behavior of the two foulant solutions on non-modified 2R surfaces was observed and their deposition curves are presented in Figure 7. As can be seen, the deposit development in the presence of protein (MOD SMUF) and in the absence of protein (SMUF) is clearly different. When only minerals are present in solution, the fouling curve increases smoothly during the whole time period considered here. When protein is present the fouling starts to be very similar to the one of SMUF but the fouling curve which initially seems to stabilize after approximately 10 hours, subsequently experiences a huge increase in the amount of fouling after around 20 hours with a trend to a new stabilization period.

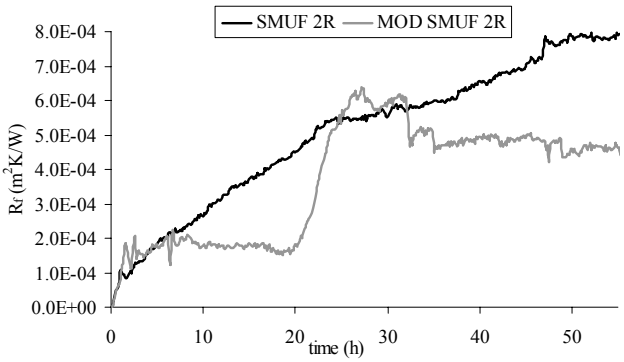

Figure 7: Different fouling behavior of SMUF and MOD SMUF on 2R (non-modified) surfaces

This difference in the fouling behavior due to the presence of protein in solution was expected based on previous work from the authors during laminar flow (Rosmaninho and Melo, submitted). It seemed, from the comparison between the two curves, that after an initial deposition, the main calcium phosphate deposit formation was delayed by the presence of protein.

This diversity in behavior enhanced the interest in analyzing the fouling behavior of the MOD SMUF solution on the different TiN surfaces in order to evaluate how the surface energy of the deposition material could affect the type of deposit build-up (see further).

To better understand the differences in the deposits formed for SMUF and MOD SMUF, both of them were observed under the scanning electron microscope (Figure 8). Calcium phosphate-based deposits with very similar individual structures were observed in the two cases (Figure 8b and 8d), but the aggregates containing protein were less defined and presented a more continuous structure than the ones without protein. In the MOD SMUF case, it is possible to see some connecting structures within the calcium phosphate aggregates, which may be responsible for a more consistently "glued" arrangement. In a macroscopic observation, the differences between them are more visible since the aggregates formed when protein was present (Figure 8a) were much smaller and also displayed a more continuous spreading throughout the surface than when only minerals were present (Figure 8c).
Nevertheless, X-ray microanalyses from both aggregates showed that their composition was mainly calcium phosphate of similar type.

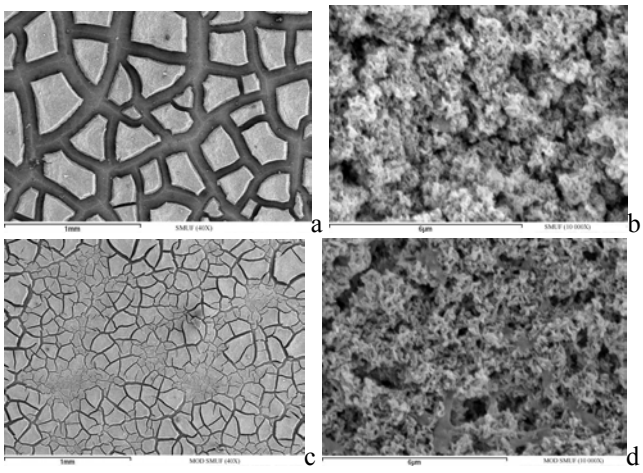

Figure 8: Deposition on 2R surfaces from SMUF solution: a) aggregates distribution (magnification 40x); b) calcium phosphate structure and MOD-SMUF solutions (magnification 10000x): c) aggregates distribution (magnification 40x); d) calcium phosphate structure (magnification 10000x)

Evolution of Bulk Properties

The evolution of the pH and the free calcium concentration in the bulk was monitored allowing to follow the progress of the reactions in the bulk as well as to compare the processes occurring.

The curves are visibly different from each other indicating differences in the bulk reactions occurring in each case. In the MOD SMUF solution, the pH suffered two big increases, the first after around 5h of deposition and the second after approximately 15h (Figure 9).

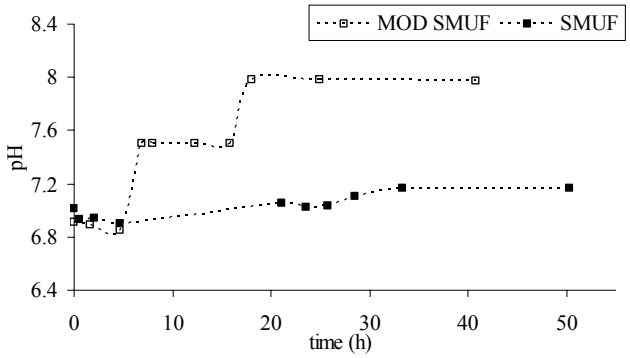

Figure 9: pH evolution of the SMUF and MOD SMUF solutions along the experiments

In the same time periods, a decrease in the free calcium concentration in the solution was observed (Figure 10). Such differences led to the conclusion that for the MOD SMUF solution the fouling process was composed of two distinct stages, each one resulting in an increase of the pH and a decrease in the free calcium concentration.

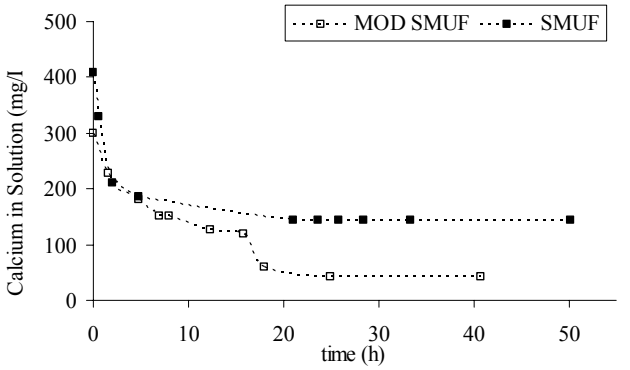

Figure 10: Concentration of calcium in solution along the experiments for SMUF and MOD SMUF solutions

These two-stage changes in both pH and calcium concentration in the bulk solution were similar in all MOD SMUF experiments, varying slightly in the time scale by no more than around one hour forward and backward.

Fouling Behavior of MOD SMUF on the Different Surfaces

All the surfaces were subjected to fouling experiments with MOD SMUF solutions and the correspondent deposit formation in time is presented in Figure 11.

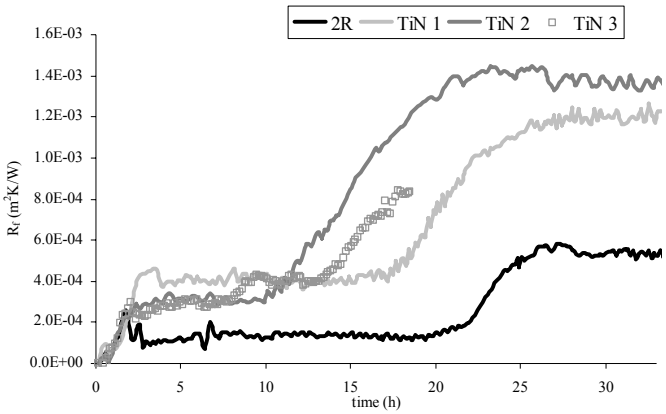

Figure 11: Fouling behavior of the MOD SMUF on the different surfaces during the deposition period

The experiment on the surface TiN 3 is only presented until around 18h of deposition since at that time, the heating system had a failure and consequently the results after that event could not be considered for analysis. However, until that time the surface was presenting a satisfactory behavior and consequently is here considered for the evaluation of the initial deposition behavior.

The fouling behavior of MOD SMUF on the unmodified stainless steel surface (2R) can clearly be distinguished from the one on the modified TiN surfaces. On the 2R surface, the first stabilization value was lower than the one for the TiN surfaces and the second increase in fouling occurs much later, with a second stabilization value for the R_f also much lower**,** indicating the presence of less deposit. One of the possible explanations for this difference between the two types of surfaces can be related to the fact that surfaces obtained by magnetic sputtering techniques tend to present higher surface roughness than the original stainless steel ones (Santos et al., 2004), and this parameter has been shown to have great importance on fouling caused both by proteins and calcium phosphate/proteins aggregates (Bansal and Chen, 2006).

The first stabilization value was achieved after approximately the same time for all the surfaces. However, the second increase in deposit started at different times depending on the surface. It was faster for the lower surface energy TiN 2 (γ- of 23) than for the intermediate surface energy TiN 3 (γ- of 46) and even faster than for the higher surface energy TiN 1 (γ- of 55). However, in every case much faster than for the 2R surface (γ- of 39), validating the statement that the fouling behavior of calcium phosphate/ protein aggregates is greatly dependent on the surface properties (simultaneously roughness and surface energy).

The explanation for this different behavior may be provided by studies presented so far on the effect of proteins on calcium phosphate deposition together with the effect of titanium-based surfaces on the deposition process (Zeng et al., 1999) even though most of those studies were done with bovine serum albumin (BSA). Other researchers showed that the adsorption of BSA has a modifying effect on the precipitation and crystallization of calcium phosphate. They also showed that the structure and the properties of the adsorbed protein layers were influenced by the deposition surface nature. Titanium (Ti) based surfaces affected the conformation of the BSA layers controlling the subsequent deposition structure of calcium phosphate (Valagão Amadeu do Serro et al., 1999; Valagão Amadeu do Serro et al., 2000; Zeng et al., 1999). Adsorption studies of BSA and calcium phosphate on TiO_2 showed that the BSA adsorption is mainly controlled by electrostatic interactions with the surface and**,** consequently**,** affected by the surface energy of the deposition material since the affinity of proteins is accepted to be higher to hydrophobic surfaces (Klinger et al., 1997; Valagão Amadeu do Serro et al., 1999; Valagão Amadeu do Serro et al., 2000). It is possible that depending on the surface, the change in conformation of the proteins and the extent of coverage of the surface is different, which may explain the difference in behavior found in this work. However, independently of the surface considered, the presence of BSA retarded the transformation process of calcium phosphate and it was suggested that the retardation on the transformation rate is due to BSA shielding of the Ca^{2+} and PO_4^{-3} sites on the growing calcium phosphate (Xie et al., 2001). Protein and calcium phosphate can co-exist in the fouling layer since the protein was found to delay the growth of the mineral component but not to inhibit its adhesion to the titanium substrata (Serro et al., 1997). The explanation for the delay observed on the fouling curves obtained in this work can be related to a similar behavior on the bulk caused by the retardation effect on the calcium phosphate crystallization process in the presence of whey protein as described by Tsuge et al. (2002).

The development of the first protein layer is dependent on the properties of the surfaces since the affinity of the proteins towards them is dependent on their surface energy. This will consequently affect the amount of deposit which will be formed. Considering the modified TiN surfaces, the

lower surface energy TiN 2 presented less deposit (smaller R_f) and the highest surface energy TiN 1 presented more deposit (higher R_f). The average value obtained for the intermediate surface energy TiN 3 was somewhere between the other two surfaces.

These layers will differ not only in the amount of deposit but also probably in the deposit structure and probably in the arrangement of the proteins. This would explain the different effects on the retardation of the second growth period and their dependency on the surface energy. The different structures developed on each surface could, therefore, explain the fact that the final amount of deposit was also dependent on the surface energy parameters of the supporting material.

CONCLUSIONS

The main conclusion drawn from this work is the importance of the surface energy of the substrate, particularly its electron-donor (γ-) component, on the fouling behavior of calcium phosphate from a simulated milk mineral solution, both in the presence as in the absence of whey proteins. More precisely:

- In the absence of whey protein, similar trends were found when relating the two fouling parameters (deposition rate and final amount of deposit) to the surface energy properties. This allowed the statement that, in general terms, calcium phosphate deposits developed on lower γ- surfaces have a slower deposition rate right from the beginning of the fouling process, are more sensitive to removal during the whole deposition process and, consequently, present less deposit at the end of the fouling period. Consequently, the introduction of surface modifications that lead to a decrease of the electron-donor surface energy component appears to be a suitable approach to obtain less deposit-prone surfaces, as far as fouling caused by milk minerals is concerned In the presence of protein in the foulant solutions, the deposition curves obtained were considerably different and two distinctive fouling growth periods were observed. The time taken until the second growth period happened was proved to be dependent on the type of surface on which fouling developed; more precisely on its roughness, surface composition and surface energy values. For these solutions, the most striking difference was found for the unmodified 2R surface, where the second growth period happened after the highest delay, as compared to all the other TiN surfaces. Among the TiN modified surfaces, however, the time required for the second growth period depended on the energy of the surfaces, since lower surface energies fouled first while higher energy surfaces fouled at last. As a consequence, the amounts of deposit formed during the first and the second stage of deposition were also different for the several surfaces tested. Consequently, and opposed to the previous case, when protein is present in the foulant solution, the best way to decrease the amount of deposit seems to be the use of unmodified stainless steel surfaces or the introduction of surface modifications that lead to an increase of the electron-donor surface energy component.

ACKNOWLEDGMENTS

The authors gratefully acknowledge the financial support of the FCT (National Science Foundation) through the PhD grant (SFRH/BD/13180/2003).

NOMENCLATURE

U	overall heat transfer coefficient	(W/m^2K)
R_f	fouling resistance	(m^2K/W)
γ^{TOT}	total solid surface energy	(mJ/m^2)
γ^{LW}	Lifshitz-van der Waals component	(mJ/m^2)
γ^{AB}	acid-base component	(mJ/m^2)
γ^-	electron donor component	(mJ/m^2)
γ^+	electron acceptor component	(mJ/m^2)
SMUF	simulated milk ultrafiltrate	
MOD SMUF	modified simulated milk ultrafiltrate	
TiN	titanium nitride	

REFERENCES

Addesso, A., and D. B. Lund, 1997, Influence of solid surface energy on protein adsorption: Journal of Food Processing and Preservation, v. 21, p. 319-333.

Bansal, B., and X. D. Chen, 2006, A Critical review of milk fouling in heat exchangers: Comprehensive Reviews in Food Science and Food Safety v. 5, p. 27-33.

Belmarbeiny, M. T., and P. J. Fryer, 1993, Preliminary Stages of Fouling from Whey-Protein Solutions: Journal of Dairy Research, v. 60, p. 467-483.

Christian, G. K., S. D. Changani, and P. J. Fryer, 2002, The effect of adding minerals on fouling from whey protein concentrate - Development of a model fouling fluid for a plate heat exchanger: Food and Bioproducts Processing, v. 80, p. 231-239.

Incropera, F. P., 1992, Fundamentals of Heat and Mass Transfer, John Wiley & Sons.

Jenness, R., and J. Koops, 1962, Preparation and properties of a salt solution which simulates milk ultrafiltrate: The Netherlands Milk and Dairy Journal, v. 16, p. 153-164.

Jeurnink, T. J. M., P. Walstra, and C. G. de Kruif, 1996, Mechanisms of fouling in dairy processing: Netherlands Milk and Dairy Journal, v. 50, p. 407-426.

Kern, D. Q., and R. E. Seaton, 1959, A Theoretical Analysis of Thermal Surface Fouling: British Chemical Engineering, v. 4, p. 258-262.

Klinger, A., D. Steinberg, D. Kohavi, and M. N. Sela, 1997, Mechanism of adsorption of human albumin to titanium in vitro: Journal of Biomedical Materials Research, v. 36, p. 387-392.

Morison, K. R., and S. H. Tie, 2002, The development and investigation of a model milk mineral fouling solution: Food and Bioproducts Processing, v. 80, p. 326-331.

Prakash, S., N. Datta, and H. C. Deeth, 2005, Methods of detecting fouling caused by heating of milk: Food Reviews International, v. 21, p. 267-293.

Rosmaninho, R., 2007, Fouling Caused by Milk Components on Modified Surfaces during Heat Treatment Processes: PhD thesis, University of Porto, Porto.

Rosmaninho, R., and L. F. Melo, 2006, Calcium phosphate deposition from simulated milk ultrafiltrate on different stainless steel-based surfaces: International Dairy Journal, v. 16, p. 81-87.

Rosmaninho, R., and L. F. Melo, submitted, Protein-calcium phosphate interactions in fouling of modified stainless steel surfaces by simulated milk: Internation Dairy Journal.

Rosmaninho, R., F. Rocha, G. Rizzo, H. Müller-Steinhagen, and L. F. Melo, accepted for publication, Calcium phosphate fouling on TiN coated stainless steel surfaces: role of ions and particles: Chemical Engineering Science.

Santos, O., T. Nylander, R. Rosmaninho, G. Rizzo, S. Yiantsios, N. Andritsos, A. Karabelas, H. Müller-Steinhagen, L. F. Melo, L. Boulange- Petermann, C. Gabet, A. Braem, C. Tragardh, and M. Paulsson, 2004, Modified stainless steel surfaces targeted to reduce fouling - surface characterization: Journal of Food Engineering, v. 64, p. 63-79.

Santos, O., T. Nylander, K. Schillen, M. Paulsson, and C. Tragardh, 2006, Effect of surface and bulk solution properties on the adsorption of whey protein onto steel surfaces at high temperature: Journal of Food Engineering, v. 73, p. 174-189.

Serro, A. P., A. C. Fernandes, B. Saramago, J. Lima, and M. A. Barbosa, 1997, Apatite deposition on titanium surfaces -- the role of albumin adsorption: Biomaterials, v. 18, p. 963-968.

Tsuge, H., Y. Tanaka, S. Yoshizawa, and T. Kuraishi, 2002, Reactive crystallization behaviour of calcium phosphate with and without whey protein addition: Chemical Engineering Research & Design, v. 80, p. 105-110.

Valagão Amadeu do Serro, A. P., A. Catarino Fernandes, B. de Jesus Vieira Saramago, and W. Norde, 1999, Bovine serum albumin adsorption on titania surfaces and its relation to wettability aspects: Journal of Biomedical Materials Research, v. 46, p. 376-381.

Valagão Amadeu do Serro, A. P., A. C. Fernandes, and B. De Jesus Vieira Saramago, 2000, Calcium phosphate deposition on titanium surfaces in the presence of fibronectin: Journal of Biomedical Materials Research, v. 49, p. 345-352.

van Oss, C. J., 1994, Interfacial forces in aqueous media: New York, USA, Marcel Dekker, Inc.

Visser, J., and T. J. M. Jeurnink, 1997, Fouling of heat exchangers in the dairy industry: Experimental Thermal and Fluid Science, v. 14, p. 407-424.

Xie, J., C. Riley, and K. Chittur, 2001, Effect of albumin on brushite transformation to hydroxyapatite: Journal of Biomedical Materials Research, v. 57, p. 357-365.

Zeng, H., K. K. Chittur, and W. R. Lacefield, 1999, Analysis of bovine serum albumin adsorption on calcium phosphate and titanium surfaces: Biomaterials, v. 20, p. 377-384.